HHS Public Access

Author manuscript

Ann N Y Acad Sci. Author manuscript; available in PMC 2020 November 01.

Published in final edited form as:

Ann N Y Acad Sci. 2019 November ; 1456(1): 44–63. doi:10.1111/nyas.14233.

In vivo identification of small molecules mediating Gpr126/Adgrg6 signaling during Schwann cell development

Ethan C. Bradley[1], **Rebecca L. Cunningham**[2], **Caroline Wilde**[3], **Rory K. Morgan**[4], **Emma A. Klug**[1], **Sophia M. Letcher**[1], **Torsten Schöneberg**[3], **Kelly R. Monk**[2,4], **Ines Liebscher**[3], **Sarah C. Petersen**[1,2]

[1]Department of Neuroscience, Kenyon College, Gambier, OH, USA

[2]Department of Developmental Biology, Washington University in St. Louis School of Medicine, St. Louis, MO, USA

[3]Rudolf Schönheimer Institute of Biochemistry, Medical Faculty, University of Leipzig, Leipzig, Germany

[4]Vollum Institute, Oregon Health & Science University, Portland, OR, USA

Abstract

Gpr126/Adgrg6, an adhesion family G protein-coupled receptor (aGPCR), is required for the development of myelinating Schwann cells in the peripheral nervous system. Myelin supports and insulates vertebrate axons to permit rapid signal propagation throughout the nervous system. In mammals and zebrafish, mutations in *Gpr126* arrest Schwann cells at early developmental stages. We exploited the optical and pharmacological tractability of larval zebrafish to uncover drugs that mediate myelination by activating Gpr126 or functioning in parallel. Using a fluorescent marker of mature myelinating glia (*Tg[mbp:EGFP-CAAX]*), we screened hypomorphic *gpr126* mutant larvae for restoration of *myelin basic protein* (*mbp*) expression along peripheral nerves following small molecule treatment. Our screens identified five compounds sufficient to promote *mbp* expression in *gpr126* hypomorphs. Using an allelic series of *gpr126* mutants, we parsed the ability of small molecules to restore *mbp*, suggesting differences in drug efficacy dependent on Schwann cell developmental state. Finally, we identify apomorphine hydrochloride as a direct small molecule activator of Gpr126 using combined *in vivo/in vitro* assays and show that aporphine class compounds promote Schwann cell development *in vivo*. Our results demonstrate the utility of *in vivo* screening for aGPCR modulators and identify small molecules that interact with the *gpr126*-mediated myelination program.

CORRESPONDING CONTACT INFORMATION Correspondence should be directed to Sarah C. Petersen, Department of Neuroscience, Kenyon College, 203 N. College Rd., Gambier, OH 43022, petersens@kenyon.edu.

AUTHOR CONTRIBUTIONS

ECB, RLC, CW, RKM, EAK, SML, IL, TS, KRM, and SCP designed experiments; ECB, RLC, CW, RKM, EAK, SML, IL, and SCP performed experiments; ECB, CW, RKM, IL, TS, KRM, and SCP analyzed results; ECB, RKM, IL, and SCP wrote the paper; all authors edited and approved of the manuscript.

COMPETING INTERESTS

The authors declare no conflicts of interest.

Keywords

adhesion GPCR; Gpr126/Adgrg6; Schwann cells; myelin; zebrafish

INTRODUCTION

Adhesion G protein-coupled receptors (aGPCRs) are the second largest class of GPCRs and facilitate proper function across different organ systems[1-3]. Within the peripheral nervous system, Gpr126/Adgrg6 is necessary for myelination, the process by which Schwann cells iteratively wrap axons to permit rapid conduction of action potentials[4-6]. Gpr126 functions cell-autonomously in myelinating Schwann cells to elevate cAMP, which drives Schwann cell wrapping in both development and regeneration[7, 8]. The necessity of Gpr126 in myelination is conserved between zebrafish and mice[9-11], illustrating the importance of Gpr126 in nervous system function across vertebrates.

Like other aGPCRs, Gpr126 has a large extracellular N-terminal fragment (NTF) which is cleaved from the 7-pass transmembrane C-terminal fragment (CTF) by the GPCR autoproteolysis-inducing (GAIN) domain at the GPCR proteolysis site (GPS)[2, 3, 12, 13]. Gpr126-CTF is sufficient for cAMP elevation via G_s protein/adenylyl cyclase pathway to activate protein kinase A, which promotes wrapping of Schwann cells around axons[7, 14]. Gpr126-NTF has multiple domains that classically promote cell-cell and cell-matrix adhesion (Figure 1A). Recently, we identified laminin-211 as a novel binding partner for Gpr126-NTF that modulates Gpr126 activation states in Schwann cell development[15]. Other ligands, collagen IV and the cellular prion protein PrP^c, are proposed to interact with the CUB/PTX domains in Gpr126-NTF[16, 17]. Interacting ligands likely regulate Gpr126-CTF signaling by mediating availability of the *Stachel*, a tethered agonist at the N terminus of Gpr126-CTF that is both necessary and sufficient for Gpr126 activation[18]. Furthermore, Gpr126-NTF is independently sufficient to mediate radial sorting, the process by which Schwann cells select and encompass a single axon segment in a 1:1 relationship. Based on our *in vivo* studies and *in vitro* assays, we predict that laminin-211 stabilizes Gpr126-NTF-CTF interaction to prevent *Stachel*-mediated activation during Gpr126-NTF-mediated radial sorting. During maturation of the Schwann cell basal lamina, laminin-211 polymerization facilitates mechanical modulation of the Gpr126-NTF or isomerization of the tethered agonist to promote *Stachel*-mediated signaling and Schwann cell myelination[15, 18].

Because GPCRs promote intracellular signaling in response to extracellular stimuli, they are superb candidate targets for pharmacological manipulation and therapeutics[19, 20]. Indeed, GPCRs have served as targets in screening compounds for myelination in the central nervous system (CNS)[21, 22]. Given its central role in multiple stages of Schwann cell development, we reasoned that Gpr126 is an informative target for identification of small molecules mediating myelination. Furthermore, because the Gpr126-mediated myelination program is conserved in zebrafish, we could perform *in vivo* pharmacological screening for small molecules that modulate Gpr126. Zebrafish larvae are a premiere model system for *in vivo* drug screening for myelin development due to their optical transparency, large numbers of embryos from a single mating event, and ability to readily absorb small molecules within

their culture water[23-25]. We previously demonstrated pharmacological activation of the Gpr126-mediated peripheral myelination program by addition of the adenylyl cyclase activator forskolin (FSK). A short pulse of FSK during development of *gpr126* mutant Schwann cells is sufficient to promote *mbp* expression and, in radially sorted Schwann cells, wrapping and myelination[6, 15]. Furthermore, Schwann cell development can be modulated in parallel to Gpr126 signaling; for instance, the ErbB2/3 receptor inhibitor AG1478 is sufficient to disrupt Schwann cell migration and differentiation in zebrafish larvae[26]. The unique utility of the system is highlighted by several screens and recently developed tools designed to identify compounds that modulate myelination in zebrafish, including those that target *gpr126*[27-33].

In the present study, we describe an unbiased small molecule drug screen in *gpr126* hypomorphs that revealed mediators of Schwann cell maturation. For rapid screening, we utilized larvae carrying a fluorescent transgenic marker of myelinating glial cells that reliably labels differentiated glial cells in the central and peripheral nervous systems[34, 35]. Our screen uncovered five compounds capable of suppressing the hypomorphic *gpr126* phenotype and restoring *mbp* expression in the periphery to different degrees. Using an established allelic series of *gpr126* zebrafish mutants[6, 15, 18], we characterized the efficacy of drugs that suppress the hypomorphic *gpr126*^{st63} phenotype and restore *mbp* expression at different stages of Schwann cell development as well as different Gpr126 signaling modalities (*e.g. Stachel* dependent or independent). From these assays, we identified and characterized apomorphine hydrochloride, an aporphine class morphine derivative, as a direct Gpr126 agonist sufficient to elevate cAMP *in vitro* and promote *mbp* expression *in vivo*. Characterization of other aporphines revealed that a related compound, glaucine, has similar ability to interact with Gpr126 and promote myelination. Our screen therefore has identified novel regulators of the Schwann cell myelination program as well as new agonistic ligands for Gpr126.

MATERIALS AND METHODS

For all assays, detailed methods are available in the supplementary material.

Zebrafish strains and husbandry

All animal experiments were performed in compliance with institutional animal protocols. Established wild-type AB*, *gpr126*^{st49} and *gpr126*^{st63} mutants[6, 36], *gpr126*^{stl47}mutants[15], *gpr126*^{stl215} mutants[18], and *Tg[mbp:EGFP-CAAX]* (*mbp:gfp*)[34] were used in this study. Zebrafish embryos were collected, raised, and staged using standard techniques[37, 38].

Primary and secondary screening in *gpr126*^{st63}*; mbp:gfp*

Schematics are provided in Figure 1G and 2G. Primary screen: *gpr126*^{st63}*; mbp:gfp* larvae were treated with 10 μM Pharmakon 1600 library (MicroSource Discovery Systems, Inc.) from 48-72 hpf. 25 μM forskolin (FSK, Sigma-Aldrich) treated at 48-53 hpf served as positive control[6]; negative controls were untreated or 1% DMSO. *mbp:gfp* in the CNS, PLLn, and motor nerves was scored at 5-6 days post-fertilization (dpf). See detailed methods for scoring criteria including hit threshold. Secondary screen: *gpr126*^{st63}*; mbp:gfp* were

treated 48-72 hpf with hit compounds from the Pharmakon library and scored as before. Compounds that met hit criteria were validated with whole-mount *in situ* hybridization (Table 1).

Small molecule treatment for *in vivo* dose-response and allelic series experiments

See detailed methods for chemical source and dilution information. Embryos were collected from heterozygous in-crosses and raised in 0.003% PTU for whole-mount *in situ* hybridization. 25-50 μM FSK served as positive control and 1% DMSO served as negative control. Other drugs and concentrations were added as indicated. Whole-mount *in situ* hybridization was performed using standard protocols[39, 40]. The *mbp* riboprobe was previously established[26]. An established PLLn scoring rubric was applied for measuring *mbp* expression[18]. For dose-response experiments with apormorphine and other aporphines, survival was recorded as the proportion of larvae alive immediately before and after drug treatment. Aporphine screening was performed in a smaller volume (2 mL), resulting in higher toxicity for apomorphine; see detailed methods. Scoring was performed with the observer blinded to genotype and treatment. Data are pooled across at least two technical replicates for each drug and allele and analyzed with GraphPad Prism.

In vitro functional assays

Full-length and Δ6bp mutant zebrafish *gpr126* constructs were cloned as described previously[18] and heterologously expressed in COS-7 cells. For cAMP accumulation assays, cells were transfected with 100 ng of plasmid using Lipofectamine™ 2000 (Thermo Fisher Scientific, Darmstadt, Germany) and incubated with concentrations of test substances. To measure cAMP concentration, the AlphaScreen cAMP assay kit (PerkinElmer Life Sciences) was used according to the manufacturer's protocol.

Imaging and analysis for aporphine compound screening

gpr126; mbp:gfp larvae were visualized at 5 dpf using a Vertebrate Automated Sorting Technology (VAST) BioImager (Union Biometrica, Holliston, MA) coupled to a spinning disc confocal microscope (SDCM) at 16X magnification (Carl Zeiss Microscopy GmbH, Jena, Germany). Maximum intensity projections were generated from z-stacks to quantify PLLn *mbp:gfp* in region of interest. See detailed methods for more information. Images were quantified with Fiji[41] and data were analyzed with GraphPad Prism.

RESULTS

A suppressor screen for *mbp:gfp* expression in *gpr126* hypomorphs

Because Gpr126 has differential and necessary roles in multiple stages of Schwann cell development, we hypothesized that we could identify small molecule modulators of peripheral myelination by screening for suppressors of $gpr126^{st63}$ hypomorphs. Several established *gpr126* zebrafish alleles result in complete abrogation of *mbp* expression ($gpr126^{stl47}$, $gpr126^{st49}$, and $gpr126^{stl215}$) due to loss of *Stachel*-mediated CTF signaling[6, 15, 18] (Figure 1A). We instead utilized the $gpr126^{st63}$ allele, which contains a lesion exchanging a conserved cysteine for tyrosine (Figure 1A) that results in reduced membrane expression, radial sorting, *mbp* expression, and myelination[15, 18]. The remainder

of the gene sequence is intact in *gpr126*^{st63} and should encode a functional NTF, complete *Stachel* sequence, and partially functional CTF sufficient to elevate cAMP to produce myelinated axons, though fewer than in wild-type. We reasoned that screening for *gpr126*^{st63} suppressor molecules would allow us to identify modulators of Schwann cell development mediated by different domains of Gpr126.

Gpr126-NTF is necessary and sufficient for radial sorting, which begins in zebrafish around 36 hpf in the posterior lateral line nerve (PLLn) (Figure 1B-C). Following radial sorting, Gpr126-CTF signals to promote *mbp* expression and wrapping around 60 hpf in the PLLn. Soon after, Schwann cells populate motor axons emanating from the spinal cord (Figure 1C). We predicted that small molecule treatment from 48-72 hpf would encompass this window and capture potential suppressor molecules that interact with *gpr126* during sorting and wrapping stages of Schwann cell development in different peripheral nerves.

To increase throughput, we observed differentiation of Schwann cells using a well-established transgenic zebrafish strain carrying membrane-tagged EGFP under the control of the *myelin basic protein* (*mbp*) promoter (*Tg[mbp:EGFP-CAAX]*, henceforth referred to as *mbp:gfp*)[34, 35]. In wild-type larvae, *mbp:gfp* is strongly expressed in the spinal cord, PLLn, and initial segments of motor nerves by 5 dpf. In contrast, *gpr126*^{st63} have substantially reduced PLLn *mbp:gfp* while maintaining strong fluorescence in the spinal cord (Figure 1D-E). We reasoned that small molecule treatment could suppress the *gpr126*^{st63}*; mbp:gfp* phenotype, restoring fluorescence in the PLLn (Figure 1F). Because motor nerve myelination commences at 4-5 dpf, it is conceivable that drugs activating Gpr126 could also promote *mbp:gfp* expression and myelination of motor nerves. In contrast, small molecules that prevent myelination would enhance the *gpr126*^{st63} phenotype, resulting in reduced peripheral *mbp:gfp*.

Given these tools and rationale, we designed a screen to test compounds in the Pharmakon 1600 library for restoration of *mbp:gfp* in *gpr126*^{st63} hypomorphs (Figure 1G). This library contains 1,600 compounds with wide structural variety that are approved for therapeutic use in humans. To screen for *gpr126*^{st63} suppressors, we generated large numbers of *gpr126*^{st63}*; mbp:gfp* embryos and arrayed the progeny into 96-well plates with three larvae per well, the maximum number that could survive the well volume. At 48 hpf, coincident with Schwann cell radial sorting, we added 10 μM library drug to each well. Larvae were incubated with drug in embryo medium for 24 hours from 48-72 hpf, encompassing the critical window for cAMP elevation and initiation of the Schwann cell terminal differentiation program. At 5-6 dpf, we scored *mbp:gfp* expression as follows: First, we ensured bright fluorescence *mbp:gfp* in the CNS to control for transgene expression. Then, we scored relative *mbp:gfp* fluorescence of the PLLn categorically as previously defined[18]. We also counted the number of motor nerves with *mbp:gfp* ventral to the horizontal myoseptum. Because central nervous system glia can myelinate the initial segment of motor axons exiting the spinal cord[42, 43] and because myelination is typically incomplete at 5-6 dpf, these could represent drugs promoting Schwann cell myelination of motor nerves. We scored samples manually because bright CNS *mbp:gfp* directly adjacent to the PNS precludes automated scoring. Manual qualitative scoring (with a dissecting stereoscope and established rubric) was ultimately

higher throughput and more consistent than quantitative scoring, which introduced methodological variability.

With these parameters, we were able to screen 1,462 drugs for suppression of the *gpr126*^{st63} hypomorphic phenotype, or 91.4% of the Pharmakon 1600 library. Of the 138 drugs not scored, 134 were lethal to all treated larvae, representing 8.4% of the total drugs screened (Supplementary Table 1). This moderate lethality rate suggests that our initial screen dose of 10 μM was appropriate to balance high hit rate with general health of screened larvae. The remaining four unscreened drugs had larvae with no transgenic fluorescence, including no expression of co-selection marker. These larvae likely exhibited transgene silencing independent of drug treatment, a common issue[44] that we observed stochastically throughout other drug treatment groups.

Identification of small molecules that restore *mbp:gfp* in *gpr126*^{st63} hypomorphs

To set a threshold for significant suppression of *gpr126*^{st63}, we analyzed *mbp:gfp* expression in control (either DMSO-treated or untreated) or 25 μM FSK-treated larvae. Control *gpr126* larvae had weak or no fluorescence along the PLLn, the location of which is marked by adjacent pigment cells along the side of the larvae (Figure 2A). In contrast, larvae treated with a moderate dose of 25 μM FSK (comparable to 10 μM dose of drugs in library) exhibit restored PLLn *mbp:gfp* due to activation of the Schwann cell differentiation program downstream of Gpr126 (Figure 2B). We scored the PLLn of negative and positive control-treated larvae by binning into categories of none, weak, some, or strong *mbp:gfp* expression and found that the vast majority (95.6%) of control larvae have weak or no fluorescence (40/113 or 35.4% “none”, 68/113 or 60.2% “weak”, Figure 2C). *mbp:gfp* expression is significantly restored in FSK-treated larvae with over half (13/22, 59.1%) scored as either some or strong *mbp:gfp* expression. We therefore called “none” and “weak” *gpr126*^{st63}-like PLLn phenotypes, while “some” and “strong” were considered non-*gpr126*^{st63}-like PLLn phenotypes ($p<0.001$, control vs. FSK, Fisher’s exact test). Because we screened a large number of drugs with relatively few larvae ($n\leq3$), we transformed these data to numerical scores to set a threshold for primary screen hits. Conversion of qualitative scores to numerical scores (none = 0, weak = 1, some = 2, strong = 3) demonstrated the significant difference between control and FSK-treated larvae (Figure 2D, 0.69±0.55 in control vs. 1.6±0.85 in FSK-treated, $p<0.001$, Student’s t-test). Finally, we found that *mbp:gfp* in motor nerves is not significantly restored with FSK treatment (Figure 2E, 0.96±1.4 in control vs. 0.73±1.1 in FSK, $p>0.45$).

With these control values, we set a hit threshold for average PLLn score and average number of *mbp:gfp*(+) motor nerves above the standard deviation for *gpr126*^{st63} controls. Primary screen drugs were counted as a “hit” if the average PLLn score across larvae ($n\leq3$) was 1.5 or greater (yellow dotted lines in Figure 2D, F), nearly the mean of FSK rescue. In addition, the presence of at least three *mbp:gfp*(+) motor nerves signified a primary screen hit (green dotted lines in Figure 2E-F) as this indicated significantly more *gfp(+)* motor axons than observed in either control treatment. With these thresholds applied, we found 98 compounds that met one or both criteria: 50 compounds (51%) had a PLLn score ≥1.5, 39 (40%) had >3 *mbp:gfp* motor nerves, and 9 (9%) met both criteria (Figure 2F).

Because of the high hit rate (98/1462, 6.7% of compounds tested), we performed a secondary screen with only hit compounds from the primary screen. We reasoned that additional rounds of screening hit compounds would ultimately remove false positives without the need for repeatedly screening the entire library. In this second round of testing, we found that treatment with 25 compounds increased PLLn score in at least one larvae and/or had an average of >3 myelinated motor nerves (Figure 2G, Table 1). We assigned functional terms to these secondary screen hits based on predicted function in PubChem (pubchem.ncbi.nlm.nih.gov/). Six hits in the secondary screen interact with GPCRs (Table 1), which represents the largest functional class in our secondary screen. Interestingly, two compounds are derivatives of morphine, naloxone hydrochloride and apomorphine hydrochloride.

Rolipram restores *mbp:gfp* in PLLn of *gpr126^{st63}* hypomorphs

As a proof-of-principle for our primary and secondary screens, we found elevated *mbp:gfp* expression in *gpr126^{st63}* larvae treated with rolipram, a selective phosphodiesterase-4 inhibitor. Rolipram treatment is sufficient to elevate Schwann cells' cAMP levels to promote myelination in mouse models[45]. Using a new stock of rolipram (*i.e.*, not from the Pharmakon library), we confirmed that PLLn *mbp:gfp* is partially restored in 10 μM rolipram-treated *gpr126^{st63}* larvae (Figure 2H, 3.6% "some" score in control vs. 25.9% "some" in rolipram-treated, $p<0.05$, Fisher's exact test). PLLn *mbp:gfp* is further restored in a dose-dependent manner with 50 μM rolipram treatment (22.9% "some" and 2.9% "strong" in 50 μM rolipram, $p<0.05$, Fisher's exact test vs. control). However, similar to FSK, rolipram treatment is insufficient to significantly elevate *mbp:gfp* in *gpr126^{st63}* motor nerves at either 10 μM (1.19±1.44 *mbp:gfp*(+) motor nerves) or 50 μM (0.94±1.1) rolipram relative to control (0.67±0.98, $p>0.05$ vs. 10 μM and vs. 50 μM, Student's t-test, Figure 2I). The identification of rolipram in our screens highlights our ability to identify small molecules that regulate cAMP in Schwann cells in an unbiased manner. Additionally, the difference in restoration of *mbp:gfp* in PLLn vs. motor nerve with rolipram treatment supports our hypothesis that cAMP elevation can promote differentiation in the PLLn, but is not sufficient to drive Schwann cell development in motor axons.

Validation of secondary screen hits in *gpr126^{st63}* hypomorphs

Based on the results of our secondary screen, we attempted to validate these hits using a different assay to visualize *mbp* expression and an independent *gpr126^{st63}* strain. We used Pharmakon 1600 library drug hits from the secondary screen to treat *gpr126^{st63}* larvae without *mbp:gfp* to ensure drug efficacy between different strains of hypomorphic mutants. In addition, we co-treated larvae with phenylthiourea (PTU) to abolish pigment formation and allow visualization of *mbp* via established whole-mount *in situ* hybridization methods[39, 40]. In our validation assay, four drugs were sufficient to elevate PLLn *mbp* in at least one of three *gpr126^{st63}* hypomorphs: telmisartan, naloxone hydrochloride, rolipram, and undecylenic acid (Table 1, Figure 3). Another small molecule hit, apomorphine hydrochloride, did not survive the validation assay, but rescue was observed in subsequent assays using new drug stock (see Figure 4). Because the mechanistic role of rolipram in Schwann cell development is established, apomorphine, telmisartan, naloxone, and undecylenic acid were selected for further study.

Prediction of direct vs. indirect *gpr126* interaction with an allelic series of *gpr126* mutants

We next considered the structure and function of hit compounds to predict whether they might function by binding/ activating Gpr126 directly (Figure 3A). Undecylenic acid is a hydrophobic fatty acid with antifungal properties; however, its mechanism of action is unknown[46, 47]. The other three hits are able to bind GPCRs, though they show diverse molecular structures (Figure 3A) and have demonstrated ability to modulate GPCRs in distinct ways. Naloxone hydrochloride is a noncompetitive opioid receptor antagonist that blocks the effects of opiates in drug overdose patients[48, 49]. Naloxone is a morphine derivative, as is another screen hit, apomorphine hydrochloride. However, apomorphine is structurally distinct from naloxone and is instead a dopamine receptor agonist sufficient to bind both D_1 and D_2-type receptors which have differential effects on cAMP production[50, 51]. Telmisartan also modulates cAMP as an antagonist for the angiotensin II type 1 receptor[52, 53]. Given the variety of screen hits, we elected to test whether they act directly on Gpr126 or in parallel/downstream using an allelic series of *gpr126* mutants.

Because *gpr126*^{st63} encodes a full-length sub-functional protein, we used three other established *gpr126* alleles with distinct phenotypes based on the lesion effect on Gpr126 structure. The strongest loss-of-function allele, *gpr126*^{stl47}, contains a Δ5+3 base pair lesion in exon 2 that produces an early STOP codon and truncates the protein in the CUB domain (Figure 1A). In *gpr126*^{stl47} mutants, Schwann cells neither radially sort nor myelinate axons[15] (Figure 3B). In contrast, both *gpr126*^{st49} and *gpr126*^{stl215} mutants have intact coding sequences for Gpr126-NTF and consequently have normal radial sorting (Figure 1A, 3B). However, *gpr126*^{st49} contains a nonsynonymous point mutation that produces a STOP codon within the GAIN domain, and therefore is predicted to lack a functional CTF to promote Schwann cell wrapping of axons. *gpr126*^{stl215} mutants have an intact CTF signaling domain with the exception of a Δ6 base pair lesion in the *Stachel* sequence that precisely deletes two amino acids necessary for *Stachel*-mediated signaling and myelination[18] (Figure 3B). In all three *gpr126* alleles, PLLn *mbp* expression is completely absent due to a failure of Gpr126 signaling, in contrast to strong *mbp* expression in wild-type (WT) and reduced expression in *gpr126*^{st63} (Figure 3C-G). Finally, *gpr126*^{st63} has an intact NTF to promote radial sorting, though decreased receptor trafficking results in less available surface NTF and reduced radial sorting[15, 18]. We therefore tested for restoration of PLLn *mbp* expression across alleles, which would allow us to infer the mechanism of drug action on Gpr126 as schematized in Figure 3B.

Undecylenic acid, naloxone hydrochloride, and telmisartan modulate *mbp* expression in parallel to Gpr126-CTF

We found that undecylenic acid is sufficient to drive *mbp* expression in radially sorted PLLn Schwann cells (Figure 3H-L). In *gpr126*^{stl47} mutants, PLLn *mbp* is absent in control and 10 μM undecylenic acid-treated larvae (Figure 3D, I). However, we observed partial restoration of *mbp* in a subset of *gpr126*^{st49} and *gpr126*^{stl215} mutants treated with 10 μM undecylenic acid (Figure 3J-K), though not to the level of *mbp* expression observed in *gpr126*^{st63} (Figure 3I). Because *gpr126*^{st49} lacks a CTF signaling domain, we concluded that undecylenic acid acts in parallel or potentially downstream of Gpr126 to promote Schwann cell *mbp* expression.

Similar results were obtained with naloxone hydrochloride (Figure 3M-Q). We observed no PLLn *mbp* in 10 μM naloxone-treated *gpr126*^{stl47} mutants (Figure 3N), but very slight suppression of *gpr126*^{st49} and *gpr126*^{stl215} (Figure 3O-P). *mbp* was observed in only one larva for each allele treated with naloxone; however, *mbp* is never observed in the PLLn of untreated mutants[6, 15, 18] and therefore suggests a small but weak level of mutant phenotype suppression. This is in contrast to *gpr126*^{st63} mutants with strong PLLn *mbp* following naloxone treatment (Figure 3Q). We therefore conclude that naloxone is a weak suppressor in *Stachel*-absent mutants and requires Schwann cell radial sorting to suppress *gpr126* mutant phenotypes.

In contrast to undecylenic acid and naloxone, we observed PLLn *mbp* expression in all alleles following telmisartan treatment (Figure 3R-U). *mbp* was weakly expressed in a subset of 5 μM telmisartan-treated *gpr126*^{stl47} (Figure 3R), *gpr126*^{st49} (Figure 3S), and *gpr126*^{stl215} (Figure 3T) mutant larvae. Because all three alleles lack a *Stachel*-containing CTF, we predict that telmisartan functions either in parallel or downstream of the *gpr126*-mediated myelination program in Schwann cells. We note that even though *gpr126*^{stl47} Schwann cells fail to undergo radial sorting, we have nonetheless observed *mbp* expression in immature *gpr126*^{stl47} Schwann cells treated with FSK[15]. Therefore, we predict that telmisartan also activates Schwann cell differentiation in the absence of both Gpr126 and radial sorting.

Apomorphine hydrochloride rescues mbp expression in *gpr126*^{st63} hypomorphs

We next tested the fourth hit from the validation assay, apomorphine hydrochloride, for its efficacy in *gpr126* suppression. Because apomorphine only weakly rescues *gpr126*^{st63} mutants at 10 μM, we tested a high dose of apomorphine (100 μM) and found it significantly restores *mbp* expression along the PLLn in 5 dpf larvae relative to DMSO-treated controls (Figure 4A-B, D), though not to the same degree as a high dose of FSK (50 μM pulse) (Figure 4C-D, 1/34 or 2.9% non-*gpr126*^{st63} phenotype in control vs. 25/25, 100% in FSK-treated, $p<0.001$ *st63*-like vs. non-*st63*-like, Fisher's exact test). Higher doses of FSK (100 μM, analogous to apomorphine) result in larval death. To identify an optimal dose of apomorphine for significant restoration of *mbp,* we performed a dose-response experiment with increasing concentrations of apomorphine in *gpr126*^{st63} larvae. We observed a dose-dependent increase of *mbp* expression in 10, 20, and 100 μM apomorphine-treated larvae, though the effect was only significant at 100 μM (Figure 4D, 4/11, 36.4% non-*gpr126*^{st63} phenotype, $p<0.05$, Fisher's exact test). However, this dose had an adverse and often lethal effect on larval development. We counted the number of larvae before and after drug treatment to measure this effect. Nearly all DMSO-treated control *gpr126*^{st63} larvae (95.6±4.2%) survive over the 24-hour treatment, and this survival rate is only slightly decreased in 10 and 20 μM (93% and 91%, respectively, Figure 4E). Only 77.8% of larvae survive overnight treatment with 50 μM apomorphine, and the most efficacious dose for *mbp* expression, 100 μM, has a survival rate of only 26.8±13% ($p<0.001$, Student's t-test). A shorter pulse of 100μM apomorphine (48-52 hpf, similar to FSK treatment) permitted larvae survival but was insufficient to restore *mbp* in *gpr126*^{st63} (data not shown). Altogether, these data show that apomorphine partially suppresses the *gpr126*^{st63} phenotype but with very similar effective and toxic concentration doses.

We also treated the allelic series of *gpr126* mutants with apomorphine to test its ability to promote *mbp* expression. Because of the high rate of lethality with an effective 100 μM dose of apomorphine, we were unable to efficiently conduct assays across all *gpr126* allelic mutants. However, we recovered enough treated *Stachel*-dead *gpr126*^{stl215} larvae to assay despite high lethality rate (30.8+36.9% with 100 μM apomorphine vs. 95.7+5.8% in controls, 97.1% in 10 μM, 93.7% in 25 μM and 92.4% in 50 μM, Figure 4F). Treatment with apomorphine resulted in reduced *mbp* expression in wild-type larvae relative to control (Figure 4G-H, K, 4/6, 66% non-strong phenotype) likely due to compromised larval health. In control-treated *gpr126*^{stl215}, we observed complete loss of *mbp* expression in the PLLn (Figure 4I, K, 0/20, 0%), in line with previous studies demonstrating that the *Stachel* tethered agonist is absolutely required to promote endogenous Gpr126 signaling in Schwann cells[18]. Critically, treatment with apomorphine partially restored *mbp* in the PLLn even though *mbp* was reduced overall. Like with *gpr126*^{st63}, we found that sub-threshold doses of apomorphine were insufficient to restore *mbp* (0/11 10 μM, 0/6 25 μM, 0/7 50 μM), while 100 μM partially restored *mbp* in the PLLn (Figure 4J, 3/10, 30% non-*gpr126*^{stl215} phenotype, $p<0.05$, Fisher's exact test vs. *gpr126*^{st63} phenotype). These data suggest that the *Stachel* sequence is dispensable for rescue of *mbp* expression by apomorphine. We conclude that apomorphine is sufficient to suppress both *gpr126*^{st63} and *gpr126*^{stl215}, though with reduced potency relative to other screen hits at a sublethal dose.

Apomorphine directly agonizes Gpr126 *in vitro*

To extend and verify the *in vivo* data, we performed *in vitro* assays to test for direct Gpr126 activation. Full-length wild-type (WT) Gpr126 expressed in COS-7 cells is sufficient to elevate cAMP compared to vector control (Figure 5A-B). Because 0.1% DMSO has an effect on cAMP levels *in vitro*, we compared substances that were solubilized in water (Figure 5A) separately from substances solubilized in DMSO (Figure 5A). Upon treatment with 100 μM apomorphine, naloxone, telmisartan, and undecylenic, significant elevation of cAMP was observed only with apomorphine (Figure 5A-B, $p<0.05$, 1-way ANOVA vs. basal activation). These data suggest that apomorphine is likely a direct activator of Gpr126, whereas the other compounds increase *mbp* in Schwann cells in a parallel or downstream pathway.

Modulation of Gpr126 activity by interacting partners (*e.g.* Laminin-211) in Schwann cells requires intact *Stachel* sequence for activation, cAMP accumulation, and *mbp* expression[15, 18], as illustrated by the *gpr126*^{stl215} allele (Figure 1A, 3B). We, therefore, expressed an analogous Δ6 base pair *Stachel* deletion Gpr126 construct (Gpr126 Δ6bp) in COS-7 cells, which shows no basal cAMP elevation, to test whether compound-mediated activation requires a functional tethered agonist. As expected, based on the WT Gpr126 data, we saw no cAMP accumulation in naloxone-, telmisartan-, or undecylenic acid-treated cells carrying Gpr126 Δ6bp. However, treatment with apomorphine significantly elevates cAMP relative to basal levels (Figure 5A, $p<0.05$, 1-way ANOVA vs. basal activation), suggesting that apomorphine agonizes Gpr126 activation independent from the *Stachel* sequence.

We also tested whether the effect of apomorphine is specific by analyzing another morphine derivative, codeine, for activation of Gpr126 and Gpr126 Δ6bp. Concentration-response

curves revealed an EC_{50} value of 94.4 μM for apomorphine on WT Gpr126 and 31.8 μM for Gpr126 Δ6bp (Figure 5C). Codeine, however, had no effect on cAMP levels in either Gpr126 construct (Figure 5D). We conclude that undecylenic acid, naloxone, and telmisartan activate the Schwann cell myelination program indirectly, while apomorphine directly and specifically activates Gpr126 independent of *Stachel* sequence to promote *mbp* expression.

The aporphine alkaloid glaucine suppresses the *gpr126^{st63}* hypomorphic phenotype

Apomorphine suppressed the *gpr126* phenotype *in vivo* (Figure 4) and directly agonized Gpr126 *in vitro* (Figure 5). Because apomorphine shares an aporphine core scaffold with alkaloid compounds, we hypothesized that other aporphine alkaloids could suppress *gpr126^{st63}* hypomorphic phenotype with reduced toxicity. We therefore selected a small set of aporphines for screening: (*R*)-nuciferine, (*S*)-glaucine, (*S*)-boldine, (*S*)-magnoflorine, and (*R*)-crebanine (Figure 6A). We first performed small-volume assays (2 mL) with these compounds to measure toxicity compared to apomorphine. Most aporphines exhibited a favorable survival rate (>80%) when incubated from 47-54 hpf with the exception of crebanine and apomorphine (at 10 μM) (Figure 6B). The increased toxicity of apomorphine in this assay is attributed to the smaller incubation volume, which exacerbated the toxicity of apomorphine with increased larval density.

The four remaining aporphines were assessed for their ability to suppress the hypomorphic phenotype in *gpr126^{st63}; mbp:gfp* (Figure 6C-G). Glaucine showed significant increase in *mbp* expression along the anterior PLLn compared to control, while the other aporphines had no effect or, for nucifierine, weak inhibition of *mbp:gfp* (Figure 6H). *mbp:gfp* expression was not significantly different with a longer incubation with glaucine (47-71 hpf, data not shown), suggesting that a short incubation window from 47-54 hpf is sufficient to suppress the *gpr126^{st63}* hypomorphic phenotype for this compound.

To determine whether glaucine might interact directly with Gpr126 like apomorphine, we assayed the ability of glaucine to suppress *gpr126^{st49}* phenotype, which encodes Gpr126-NTF but has a premature stop precluding expression of the Gpr126-CTF signaling domain (Figure 3). We observe that glaucine fails to suppress the *gpr126^{st49}* phenotype (Figure 6I, J), with no PLLn *mbp:gfp* in *gpr126^{st49}* larvae treated with glaucine (50 μM) from 47-54 hpf. As a positive control, we added 50 μM forskolin, a known small-molecule suppressor of the *gpr126^{st49}* phenotype, and saw partial restoration of *mbp:gfp* expression (Figure 6K). Therefore, we predict glaucine, like apomorphine, acts directly with Gpr126 to promote cAMP elevation and Schwann cell differentiation *in vivo.*

DISCUSSION

Gpr126 mediates multiple stages of Schwann cell development by virtue of its NTF-CTF interactions and binding of endogenous ligands[6, 10, 15, 16, 18]. In the present study, we designed a medium-throughput screen in zebrafish to identify small molecules that interact with the *gpr126*-mediated myelination program. By observing *mbp:gfp* in *gpr126* hypomorphs treated with 1,600 small molecules in the Pharmakon library, we discovered four novel compounds that suppress the *gpr126* hypomorph phenotype and partially restore Schwann cell differentiation. Structure-function characterization using an allelic series of

gpr126 mutants demonstrates that modulation of the myelination program is dependent upon Schwann cell developmental state. In addition, we discovered that apomorphine hydrochloride, a morphine derivative and dopamine receptor agonist, directly activates Gpr126 in a *Stachel*-independent manner.

Small molecule screens for regulators of adhesion family GPCRs

Autocatalytic processing of aGPCRs into NTF and CTF and production of the tethered *Stachel* agonist permits subfunctionalization of receptor domains[2, 15, 54, 55]. aGPCRs have complex potential to mediate intracellular signal transduction; however, few studies have identified compounds that can perturb aGPCR signaling. Recently, an *in vitro* screen specifically targeted Gpr56/Adgrg1 and identified dihydromunduletone as a selective antagonist that also antagonizes Gpr114/Adgrg5[56]. Both Gpr56 and Gpr114 are members of the same structural group as Gpr126, Class VIII, which have alike and promiscuous *Stachel* sequences[57, 58]. Similarly, a small-scale *in vitro* screen across a variety of aGPCRs identified beclomethasone diproprionate as an agonist for Adgrg3/Gpr97, another Class VIII aGPCR[59]. Although *in vivo* screening in our study is lower throughput than *in vitro* assays, it offers an attractive complementary approach to find bona fide small molecules interacting with aGPCRs to promote signaling and cellular function.

Myelinating glia in the CNS express multiple druggable targets, including aGPCRs Gpr56/Adgrg1 and Gpr98/Adgrv1 in oligodendrocyte lineage cells[60]. In mouse and zebrafish *gpr56* mutants, oligodendrocyte precursor cells precociously exit the earlier developmental state and result in fewer myelin sheaths[61, 62]. In contrast, Gpr98 appears to stabilize the mature state of oligodendrocytes, as loss of *Gpr98* results in decreased expression of myelin associated glycoprotein (MAG), a mature oligodendrocyte marker[63]. Therefore, small molecule modulators of Gpr56 and Gpr98 have the potential to restore proper myelination in disease or injury states in the CNS. Our screen serves as a proof-of-principle for identification of therapeutic compounds that target aGPCRs to restore myelination.

Small molecule screens for regulators of glial cell development and myelination

Our screen builds upon previous *in vitro*[64, 65] and *in vivo*[25, 31, 32] screens to identify small molecules promoting glial cell development. Much of the focus has been on restoration of CNS myelin via oligodendrocytes. In contrast, relatively few screens have studied peripheral myelination *in vivo*. One limitation is the difficulty in screening fluorescence in the periphery of zebrafish (*e.g.*, PLLn or motor nerves) adjacent to the strong transgenic fluorescence in the CNS. The development of more powerful high-throughput analyses of fluorescence and development of new markers may overcome this technical limitation[28, 31]. Furthermore, we observed that PLLn *mbp* was more easily restored relative to motor nerves in both fluorescent and *in situ* hybridization assays, suggesting cAMP elevation alone is not sufficient to restore *mbp* expression in *gpr126* motor axons with treatment up to 72 hpf. This disparity could be due to differences in the nerve structure or function or differences in the populations of Schwann cell precursors along these nerves. Alternatively, we observe few Schwann cells ventral to the horizontal myoseptum at our timepoints (data not shown), thus we may not observe substantial rescue because too few Schwann cells are present.

Another *gpr126* suppressor screen was recently performed using different hypomorphic and loss-of-function alleles and took advantage *gpr126* function in the ear[33]. Rather than a fluorescent marker, this screen used whole-mount *in situ* hybridization in both ear and PLLn. Of 3120 molecules tested, this screen yielded 41 molecules rescuing *mbp* in the PLLn of *gpr126* hypomorphs, with 19 predicted to interact directly with Gpr126 based on suppression of a strong *gpr126* allele that lacks CTF function (see rationale in Figure 3). Importantly, this screen was conducted at 60-90 hpf versus our primary screen at 48-72 hpf, which reflects difference in ear developmental stages compared to earlier Gpr126 function in PLLn Schwann cells. Furthermore, while our assay investigated the PLLn in the primary screen, this study tested PLLn *mbp* in a secondary assay following a primary screen for otic *versican b (vcanb).* These differences in timing and tissue-specificity likely underlies differences in hits. Our screen primarily uncovered GPCR interactors with morphine-like structures, whereas the other screen recovered calcium channel agonist and antagonists, particularly with dihydropyridine structure. These contrasting hits could distinguish tissue-specific activation mechanisms for Gpr126, as compounds that did not rescue otic *gpr126* function would not have been screened in the PLLn. Similarly, we did not see otic vesicle swelling suppression with any of the drugs in our screen with treatment at 48-72 hpf (data not shown). Future studies can parse hits from these screens on Gpr126 function at differing developmental stages, or for interaction with *gpr56/adgrg1*, which is also necessary for proper peripheral myelin development and maintenance[66].

Models for drug action based on influence of Schwann cell developmental state

Gpr126-NTF is required for radial sorting in Schwann cells, though the mechanism by which it intracellularly transduces this cue is unclear[15]. Our allelic series analyses suggest that undecylenic acid and naloxone are sufficient to promote *mbp* expression specifically in Schwann cells that are predicted to express Gpr126-NTF and naloxone cannot activate the differentiation program in immature Schwann cells until radial sorting is underway (Figure 3). Undecylenic acid is an antifungal drug without defined receptors[47] and thus the nature of activation, and whether it is Schwann cell-autonomous, remains unclear. The mechanism of action may involve a receptor either exclusively expressed in Schwann cells following radial sorting, or one acting non-cell-autonomously as an instructive cue for myelination by pre-myelinating Schwann cells (*e.g.*, as an axonal ligand).

In contrast, naloxone is a well-studied opioid receptor antagonist routinely used to block the effects of opiate overdoses. Opioid receptors are expressed in terminals and processes of sensory and nociceptive neurons[67] and promote myelination in cultured oligodendrocytes[65], but their expression in Schwann cells is not established. Thus, one model is a non-cell-autonomous effect on Schwann cells mediated by the axons they myelinate. However, the low level of rescue in *gpr126*^{st49} and *gpr126*^{stl215} hints at potential indirect and direct Gpr126 activation by naloxone specifically in pre-myelinating Schwann cells. We previously found that Laminin-211 suppresses cAMP accumulation in static Gpr126-expressing cultures, but nonetheless acts to elevate cAMP in dynamic *in vitro* assays and *in vivo*[15]. Similarly, we do not observe cAMP accumulation in static naloxone-treated Gpr126-expressing cells *in vitro* (Figure 5). Therefore, naloxone may act in two ways: indirectly via

opioid receptors on adjacent axons, and by cell-autonomous activation of Gpr126 in dynamic and later-developing states.

The angiotensin II type 1 (AT) receptor antagonist, telmisartan, was sufficient to promote *mbp* expression across all *gpr126* alleles, even *gpr126*^{stl47} which lacks a functional Gpr126-NTF and thus fails to radially sort peripheral axons. AT receptors are upregulated in functional recovery of injured peripheral nerves[68], and telmisartan treatment improves peripheral nerve regeneration[69]. However, the expression of AT receptors in Schwann cells is not established and the cell autonomy of telmisartan's action is unclear. Notably, AT_1 receptors are coupled to $G_{q/11}$ and G_i and would therefore inhibit the production of cAMP[70]. Telmisartan as an AT receptor antagonist should then increase or at least stabilize cAMP levels. However, we observe a reduction of basal GPR126-induced cAMP levels, which indicates additional AT receptor-independent effect of telmisartan. We have previously observed that cAMP elevation by FSK is sufficient to promote *mbp* expression in *gpr126*^{stl47} mutants in a similar fashion; however, FSK-treated *gpr126*^{stl47} mutants still fail to complete radial sorting and express terminal differentiation markers in the absence of myelin[15]. Further investigation into telmisartan's mechanism of action can include both the target receptor as well as whether receptor activation mediates radial sorting and wrapping in addition to *mbp* expression.

Apomorphine directly activates Gpr126-mediated cAMP accumulation

In addition to compounds that act in parallel to or potentially downstream of *gpr126*, our study revealed a novel direct activator of Gpr126, apomorphine hydrochloride. Due to high lethality with efficacious doses, we could not dissect the ability of apomorphine to rescue *mbp* expression across all *gpr126* alleles. However, our *in vivo* assays demonstrate that apomorphine promotes *mbp* expression in *Stachel*-dead *gpr126*^{stl215} mutants, suggesting a *Stachel*-independent mode of action (Figure 4). While we cannot formally exclude a Gpr126-independent mechanism *in vivo,* we favor a model in which apomorphine directly agonizes Gpr126-CTF in Schwann cells to promote *mbp* expression, rather than via apomorphine's established role agonizing G_i-coupled D_2 dopamine receptors[71]. In the latter case, activation of D_2 receptors in Schwann cells would result in reduction of cAMP, which would normally prevent Schwann cell differentiation and *mbp* expression. Thus, we conclude that apomorphine directly activates Gpr126 *in vivo*, a model which is corroborated by our heterologous *in vitro* assays showing apomorphine directly activates both wild-type *and Stachel*-dead Gpr126 (Figure 5). Our previous work showed *Stachel*-mediated activation is facilitated by dynamic assays and suggested physical dissociation of Gpr126-NTF could liberate the cryptic tethered agonist[13, 15, 18] . In the present study, the elevation of cAMP in static cultures suggests a bypass of mechanical activation of Gpr126 and direct activation of G_s signaling upon apomorphine binding to the Gpr126-CTF. To our knowledge, our study is the first to demonstrate activation of Gpr126 signaling in a *Stachel*-independent fashion.

Intriguingly, two hits in our screen, apomorphine and naloxone, are both morphine derivatives with different structures and pharmacologic effects. Importantly, apomorphine does not bind opioid receptors, whereas naloxone is an opioid receptor antagonist. We decided to include codeine, an agonist of opioid receptors to test specificity and found only

apomorphine is sufficient to elevate cAMP in Gpr126-expressing cells (Figure 5). To investigate if this effect is specific to apomorphine *in vivo*, we treated *gpr126*^{st63} hypomorphs and *gpr126*^{st49} NTF-only mutants with related alkaloids. We found that one of these aporphines, glaucine, suppresses the *gpr126*^{st63} hypomorphic phenotype. Glaucine, like apomorphine, interacts with dopamine receptors, but can also modulate serotonergic receptors and intriguingly interacts with L-type Ca^{2+} channels *in vitro*[72-74], mirroring the findings of another *gpr126* suppressor screen[33]. However, glaucine did not suppress *gpr126*^{st49}, suggesting that it also functions specifically through *gpr126* as a direct agonist like apomorphine (Figure 6).

Taken together, our screen demonstrates the feasibility of identifying pharmacological modulators of aGPCRs that interact directly with the receptor or act in parallel pathways. Because the functions of aGPCRs span many tissue types, we emphasize the ability to perform similar *in vivo* small molecule screens for other aGPCRs using the larval zebrafish model. Finally, our study revealed five novel small molecule regulators of Schwann cell development that act at different points in the differentiation pathway. These compounds represent an exciting opportunity to dissect the basic biology of Schwann cell development and develop therapeutics for neurological disorders by targeting Gpr126 and other GPCRs.

Supplementary Material

Refer to Web version on PubMed Central for supplementary material.

ACKNOWLEDGEMENTS

We thank Steve Johnson, Lila Solnica-Krezel, John Hofferberth, and members of the Monk and Petersen laboratories for valuable discussions and feedback. We thank Becky Gallagher and the Animal Care staff at Kenyon College as well as Charleen Johnson and the Washington University Zebrafish Consortium staff for excellent zebrafish care. This work was supported by Kenyon College Summer Scholars fellowships to EB; National Science Foundation Graduate Research Fellowship DGE-1745038 to RLC, the junior research grant by the Medical Faculty of the University of Leipzig to CW, a Collins Medical Trust grant to RKM, the German Research Foundation (Research Unit FOR 2149, project numbers: 266022790/266061011; CRC 1052 B06, project number: 209933838) to TS and IL, the BMBF (IFB AdipositasDiseases Leipzig AD2-7102) and the European Social Fund and the Free State of Saxony to IL; NIH R01 NS079445 and NIH R01 HD080601 to KRM; and an Integrative Research in Pharmacology fellowship from the American Society for Pharmacology and Experimental Therapeutics (ASPET-IRP) to SCP. SCP accepts responsibility for data analysis integrity.

REFERENCES

1. Arac D, Aust G, Calebiro D, et al. 2012 Dissecting signaling and functions of adhesion G protein-coupled receptors. Annals of the New York Academy of Sciences. 1276: 1–25. [PubMed: 23215895]
2. Langenhan T, Aust G & Hamann J. 2013 Sticky signaling--adhesion class G protein-coupled receptors take the stage. Science signaling. 6: re3. [PubMed: 23695165]
3. Bjarnadottir TK, Fredriksson R & Schioth HB. 2007 The adhesion GPCRs: a unique family of G protein-coupled receptors with important roles in both central and peripheral tissues. Cellular and molecular life sciences : CMLS. 64: 2104–2119. [PubMed: 17502995]
4. Jessen KR & Mirsky R. 2005 The origin and development of glial cells in peripheral nerves. Nat Rev Neurosci. 6: 671–682. [PubMed: 16136171]
5. Woodhoo A & Sommer L. 2008 Development of the Schwann cell lineage: from the neural crest to the myelinated nerve. Glia. 56: 1481–1490. [PubMed: 18803317]

6. Monk KR, Naylor SG, Glenn TD, et al. 2009 A G protein-coupled receptor is essential for Schwann cells to initiate myelination. Science. 325: 1402–1405. [PubMed: 19745155]
7. Mogha A, Benesh AE, Patra C, et al. 2013 Gpr126 functions in Schwann cells to control differentiation and myelination via G-protein activation. The Journal of neuroscience : the official journal of the Society for Neuroscience. 33: 17976–17985. [PubMed: 24227709]
8. Mogha A, Harty BL, Carlin D, et al. 2016 Gpr126/Adgrg6 Has Schwann Cell Autonomous and Nonautonomous Functions in Peripheral Nerve Injury and Repair. J Neurosci. 36: 12351–12367. [PubMed: 27927955]
9. Ackerman SD & Monk KR. 2016 The scales and tales of myelination: using zebrafish and mouse to study myelinating glia. Brain Res. 1641: 79–91. [PubMed: 26498880]
10. Monk KR, Oshima K, Jors S, et al. 2011 Gpr126 is essential for peripheral nerve development and myelination in mammals. Development. 138: 2673–2680. [PubMed: 21613327]
11. Lyons DA & Talbot WS. 2014 Glial cell development and function in zebrafish. Cold Spring Harb Perspect Biol. 7: a020586. [PubMed: 25395296]
12. Liebscher I, Ackley B, Araç D, et al. 2014 New functions and signaling mechanisms for the class of adhesion G protein-coupled receptors. Ann N Y Acad Sci. 1333: 43–64. [PubMed: 25424900]
13. Arac D, Boucard AA, Bolliger MF, et al. 2012 A novel evolutionarily conserved domain of cell-adhesion GPCRs mediates autoproteolysis. EMBO J. 31: 1364–1378. [PubMed: 22333914]
14. Glenn TD & Talbot WS. 2013 Analysis of Gpr126 function defines distinct mechanisms controlling the initiation and maturation of myelin. Development. 140: 3167–3175. [PubMed: 23804499]
15. Petersen SC, Luo R, Liebscher I, et al. 2015 The Adhesion GPCR GPR126 Has Distinct, Domain-Dependent Functions in Schwann Cell Development Mediated by Interaction with Laminin-211. Neuron. 85: 755–769. [PubMed: 25695270]
16. Küffer A, Lakkaraju AK, Mogha A, et al. 2016 The prion protein is an agonistic ligand of the G protein-coupled receptor Adgrg6. Nature. 536: 464–468. [PubMed: 27501152]
17. Paavola KJ, Sidik H, Zuchero JB, et al. 2014 Type IV collagen is an activating ligand for the adhesion G protein-coupled receptor GPR126. Science signaling. 7: ra76. [PubMed: 25118328]
18. Liebscher I, Schon J, Petersen SC, et al. 2014 A tethered agonist within the ectodomain activates the adhesion G protein-coupled receptors GPR126 and GPR133. Cell reports. 9: 2018–2026. [PubMed: 25533341]
19. Jacobson KA 2015 New paradigms in GPCR drug discovery. Biochem Pharmacol. 98: 541–555. [PubMed: 26265138]
20. Miao Y & McCammon JA. 2016 G-protein coupled receptors: advances in simulation and drug discovery. Curr Opin Struct Biol. 41: 83–89. [PubMed: 27344006]
21. Hennen S, Wang H, Peters L, et al. 2013 Decoding signaling and function of the orphan G protein-coupled receptor GPR17 with a small-molecule agonist. Sci Signal. 6: ra93. [PubMed: 24150254]
22. Lu C, Dong L, Zhou H, et al. 2018 G-Protein-Coupled Receptor Gpr17 Regulates Oligodendrocyte Differentiation in Response to Lysolecithin-Induced Demyelination. Sci Rep. 8: 4502. [PubMed: 29540737]
23. Zon LI & Peterson RT. 2005 In vivo drug discovery in the zebrafish. Nature reviews. Drug discovery. 4: 35–44. [PubMed: 15688071]
24. D'Rozario M, Monk KR & Petersen SC. 2017 Analysis of myelinated axon formation in zebrafish. Methods Cell Biol. 138: 383–414. [PubMed: 28129853]
25. Buckley CE, Goldsmith P & Franklin RJ. 2008 Zebrafish myelination: a transparent model for remyelination? Dis Model Mech. 1: 221–228. [PubMed: 19093028]
26. Lyons DA, Pogoda HM, Voas MG, et al. 2005 erbb3 and erbb2 are essential for schwann cell migration and myelination in zebrafish. Curr Biol. 15: 513–524. [PubMed: 15797019]
27. Preston MA & Macklin WB. 2015 Zebrafish as a model to investigate CNS myelination. Glia. 63: 177–193. [PubMed: 25263121]
28. Preston MA, Finseth LT, Bourne JN, et al. 2019 A novel myelin protein zero transgenic zebrafish designed for rapid readout of in vivo myelination. Glia.

29. Buckley CE, Marguerie A, Roach AG, et al. 2010 Drug reprofiling using zebrafish identifies novel compounds with potential pro-myelination effects. Neuropharmacology. 59: 149–159. [PubMed: 20450924]
30. Cole KLH, Early JJ & Lyons DA. 2017 Drug discovery for remyelination and treatment of MS. Glia. 65: 1565–1589. [PubMed: 28618073]
31. Early JJ, Cole KL, Williamson JM, et al. 2018 An automated high-resolution in vivo screen in zebrafish to identify chemical regulators of myelination. Elife. 7.
32. Kazakova N, Li H, Mora A, et al. 2006 A screen for mutations in zebrafish that affect myelin gene expression in Schwann cells and oligodendrocytes. Dev Biol. 297: 1–13. [PubMed: 16839543]
33. Diamantopolou E, Baxendale S, de la Vega de Léon A, et al. 2019 Identification of compounds that rescue otic and myelination defects in the zebrafish adgrg6 (gpr126) mutant. eLife. 520056.
34. Almeida RG, Czopka T, Ffrench-Constant C, et al. 2011 Individual axons regulate the myelinating potential of single oligodendrocytes in vivo. Development. 138: 4443–4450. [PubMed: 21880787]
35. Czopka T & Lyons DA. 2011 Dissecting mechanisms of myelinated axon formation using zebrafish. Methods in cell biology. 105: 25–62. [PubMed: 21951525]
36. Pogoda HM, Sternheim N, Lyons DA, et al. 2006 A genetic screen identifies genes essential for development of myelinated axons in zebrafish. Dev Biol. 298: 118–131. [PubMed: 16875686]
37. Westerfield M 2000 The Zebrafish Book: A Guide for the Laboratory Use of Zebrafish (Danio Rerio) Institute of Neuroscience. University of Oregon.
38. Kimmel CB, Ballard WW, Kimmel SR, et al. 1995 Stages of embryonic development of the zebrafish. Developmental dynamics : an official publication of the American Association of Anatomists. 203: 253–310. [PubMed: 8589427]
39. Cunningham RL & Monk KR. 2018 Whole Mount In Situ Hybridization and Immunohistochemistry for Zebrafish Larvae. Methods Mol Biol. 1739: 371–384. [PubMed: 29546721]
40. Thisse C & Thisse B. 2008 High-resolution in situ hybridization to whole-mount zebrafish embryos. Nat Protoc. 3: 59–69. [PubMed: 18193022]
41. Schindelin J, Arganda-Carreras I, Frise E, et al. 2012 Fiji: an open-source platform for biological-image analysis. Nat Methods. 9: 676–682. [PubMed: 22743772]
42. Kucenas S, Wang WD, Knapik EW, et al. 2009 A selective glial barrier at motor axon exit points prevents oligodendrocyte migration from the spinal cord. J Neurosci. 29: 15187–15194. [PubMed: 19955371]
43. Smith CJ, Morris AD, Welsh TG, et al. 2014 Contact-mediated inhibition between oligodendrocyte progenitor cells and motor exit point glia establishes the spinal cord transition zone. PLoS Biol. 12: e1001961. [PubMed: 25268888]
44. Goll MG, Anderson R, Stainier DY, et al. 2009 Transcriptional silencing and reactivation in transgenic zebrafish. Genetics. 182: 747–755. [PubMed: 19433629]
45. Guo L, Moon C, Niehaus K, et al. 2012 Rac1 controls Schwann cell myelination through cAMP and NF2/merlin. J Neurosci. 32: 17251–17261. [PubMed: 23197717]
46. Petrović M, Bonvin D, Hofmann H, et al. 2018 Fungicidal PMMA-Undecylenic Acid Composites. Int J Mol Sci. 19.
47. Shi D, Zhao Y, Yan H, et al. 2016 Antifungal effects of undecylenic acid on the biofilm formation of Candida albicans. Int J Clin Pharmacol Ther. 54: 343–353. [PubMed: 26902505]
48. Kerensky T & Walley AY. 2017 Opioid overdose prevention and naloxone rescue kits: what we know and what we don't know. Addiction science & clinical practice. 12: 4. [PubMed: 28061909]
49. Snyder SH & Childers SR. 1979 Opiate receptors and opioid peptides. Annual review of neuroscience. 2: 35–64.
50. Beaulieu J-M & Gainetdinov RR. 2011 The physiology, signaling, and pharmacology of dopamine receptors. Pharmacological reviews. 63: 182–217. [PubMed: 21303898]
51. Chipkin RE, McQUADE RD & Iorio LC. 1987 D1 and D2 dopamine binding site up-regulation and apomorphine-induced stereotypy. Pharmacology Biochemistry and Behavior. 28: 477–482.

52. Benson SC, Pershadsingh HA, Ho CI, et al. 2004 Identification of telmisartan as a unique angiotensin II receptor antagonist with selective PPARgamma-modulating activity. Hypertension. 43: 993–1002. [PubMed: 15007034]
53. Michel MC, Foster C, Brunner HR, et al. 2013 A systematic comparison of the properties of clinically used angiotensin II type 1 receptor antagonists. Pharmacological reviews. 65: 809–848. [PubMed: 23487168]
54. Promel S, Frickenhaus M, Hughes S, et al. 2012 The GPS Motif Is a Molecular Switch for Bimodal Activities of Adhesion Class G Protein-Coupled Receptors. Cell reports. 2: 321–331. [PubMed: 22938866]
55. Patra C, van Amerongen MJ, Ghosh S, et al. 2013 Organ-specific function of adhesion G protein-coupled receptor GPR126 is domain-dependent. Proceedings of the National Academy of Sciences of the United States of America. 110: 16898–16903. [PubMed: 24082093]
56. Stoveken HM, Bahr LL, Anders MW, et al. 2016 Dihydromunduletone Is a Small-Molecule Selective Adhesion G Protein-Coupled Receptor Antagonist. Mol Pharmacol. 90: 214–224. [PubMed: 27338081]
57. Harty BL, Krishnan A, Sanchez NE, et al. 2015 Defining the gene repertoire and spatiotemporal expression profiles of adhesion G protein-coupled receptors in zebrafish. BMC Genomics. 16: 62. [PubMed: 25715737]
58. Demberg LM, Winkler J, Wilde C, et al. 2017 Activation of Adhesion G Protein-coupled Receptors: AGONIST SPECIFICITY OF STACHEL SEQUENCE-DERIVED PEPTIDES. J Biol Chem. 292: 4383–4394. [PubMed: 28154189]
59. Gupte J, Swaminath G, Danao J, et al. 2012 Signaling property study of adhesion G-protein-coupled receptors. FEBS Lett. 586: 1214–1219. [PubMed: 22575658]
60. Mogha A, D'Rozario M & Monk KR. 2016 G protein-coupled receptors in myelinating glia. Trends in pharmacological sciences. 37: 977–987. [PubMed: 27670389]
61. Ackerman SD, Garcia C, Piao X, et al. 2015 The adhesion GPCR Gpr56 regulates oligodendrocyte development via interactions with Gα12/13 and RhoA. Nat Commun. 6: 6122. [PubMed: 25607772]
62. Giera S, Deng Y, Luo R, et al. 2015 The adhesion G protein-coupled receptor GPR56 is a cell-autonomous regulator of oligodendrocyte development. Nat Commun. 6: 6121. [PubMed: 25607655]
63. Shin D, Lin S-T, Fu Y-H, et al. 2013 Very large G protein-coupled receptor 1 regulates myelin-associated glycoprotein via Gαs/Gαq-mediated protein kinases A/C. Proceedings of the National Academy of Sciences. 110: 19101–19106.
64. Mei F, Fancy SP, Shen YA, et al. 2014 Micropillar arrays as a high-throughput screening platform for therapeutics in multiple sclerosis. Nature medicine. 20: 954–960.
65. Mei F, Mayoral SR, Nobuta H, et al. 2016 Identification of the Kappa-Opioid Receptor as a Therapeutic Target for Oligodendrocyte Remyelination. J Neurosci. 36: 7925–7935. [PubMed: 27466337]
66. Ackerman SD, Luo R, Poitelon Y, et al. 2018 GPR56/ADGRG1 regulates development and maintenance of peripheral myelin. J Exp Med. 215: 941–961. [PubMed: 29367382]
67. Mambretti EM, Kistner K, Mayer S, et al. 2016 Functional and structural characterization of axonal opioid receptors as targets for analgesia. Mol Pain. 12.
68. Gallinat S, Yu M, Dorst A, et al. 1998 Sciatic nerve transection evokes lasting up-regulation of angiotensin AT2 and AT1 receptor mRNA in adult rat dorsal root ganglia and sciatic nerves. Brain Res Mol Brain Res. 57: 111–122. [PubMed: 9630555]
69. Yuksel TN, Halici Z, Demir R, et al. 2015 Investigation of the effect of telmisartan on experimentally induced peripheral nerve injury in rats. Int J Neurosci. 125: 464–473. [PubMed: 25069044]
70. Higuchi S, Ohtsu H, Suzuki H, et al. 2007 Angiotensin II signal transduction through the AT1 receptor: novel insights into mechanisms and pathophysiology. Clinical science. 112: 417–428. [PubMed: 17346243]
71. Usiello A, Baik JH, Rougé-Pont F, et al. 2000 Distinct functions of the two isoforms of dopamine D2 receptors. Nature. 408: 199–203. [PubMed: 11089973]

72. Asencio M, Hurtado-Guzmán C, López JJ, et al. 2005 Structure–affinity relationships of halogenated predicentrine and glaucine derivatives at D1 and D2 dopaminergic receptors: halogenation and D1 receptor selectivity. Bioorganic & medicinal chemistry. 13: 3699–3704. [PubMed: 15862999]

73. Heng HL, Chee CF, Thy CK, et al. 2019 In vitro functional evaluation of isolaureline, dicentrine and glaucine enantiomers at 5-HT2 and α1 receptors. Chemical biology & drug design. 93: 132–138. [PubMed: 30216681]

74. Cortijo J, Villagrasa V, Pons R, et al. 1999 Bronchodilator and anti-inflammatory activities of glaucine: In vitro studies in human airway smooth muscle and polymorphonuclear leukocytes. British journal of pharmacology. 127: 1641–1651. [PubMed: 10455321]

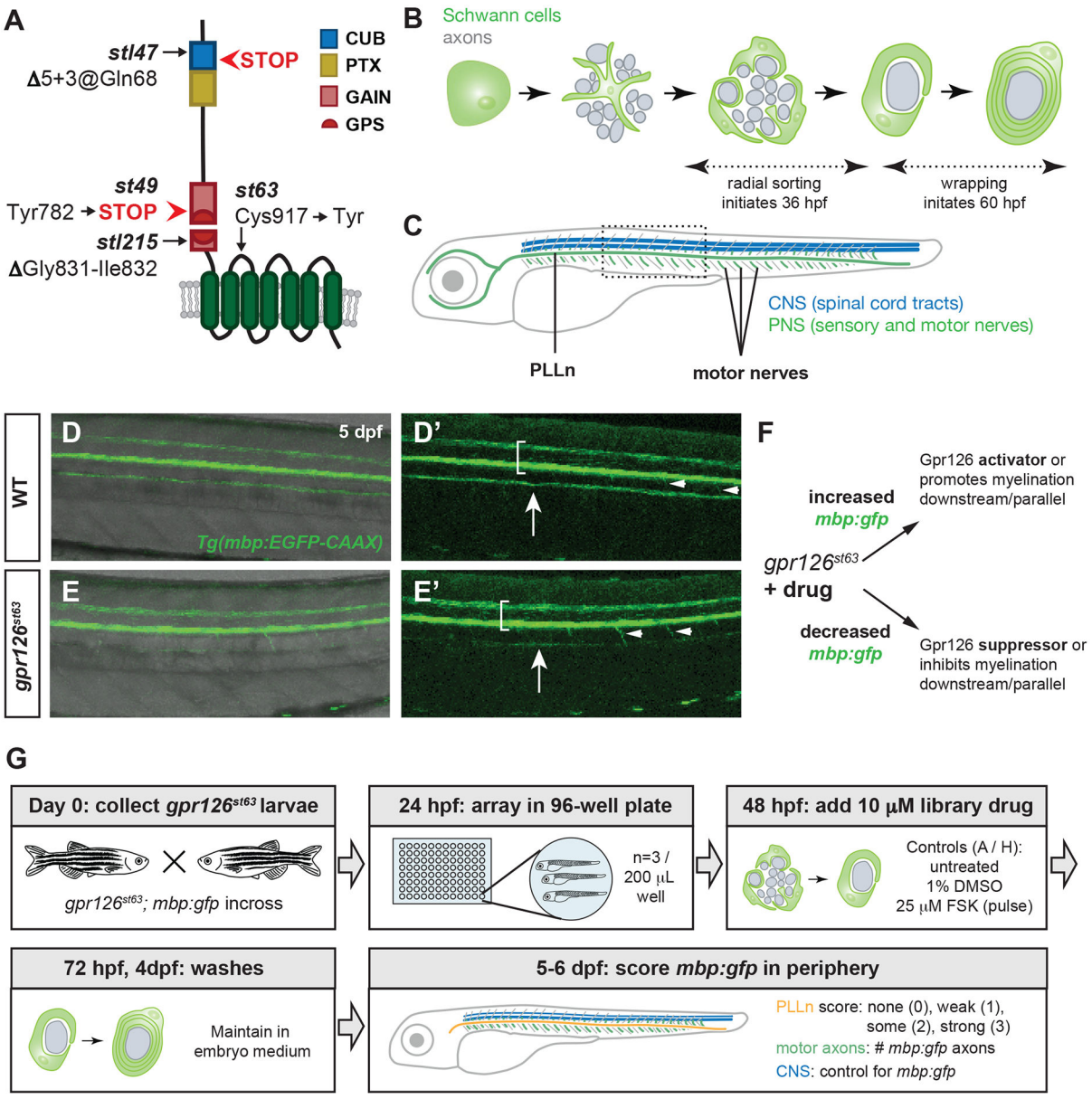

Figure 1. A small molecule suppressor screen in *gpr126* hypomorphs for compounds that promote Schwann cell differentiation

(**A**) Schematic of zebrafish Gpr126 protein and mutant alleles. (**B**) Schematic of zebrafish Schwann cell development (green) around axons (gray) in cross-section. Radial sorting begins around 36 hours post-fertilization (hpf); wrapping is observed by 60 hpf. (**C**) Schematic of 5-6 days post-fertilization (dpf) larval zebrafish with central nervous system (CNS) myelin (blue) and myelinated nerves in the peripheral nervous system (PNS) (green). PLLn = posterior lateral line nerve. Boxed region shown in panels **D**-**E**. (**D**-**E**) *Tg(mbp:EGFP-CAAX)* expression (henceforth *mbp:gfp*) in wild-type (WT) and *gpr126*^{st63} larvae at 5 dpf. Brackets denote spinal cord, arrows indicate PLLn, arrowheads mark emerging motor axons. Note strong *mbp:gfp* expression in the PLLn of WT (**D**-**D'**) but

reduced expression in *gpr126*^{st63} PLLn (**E-E'**). (**F**) Logic of *gpr126*^{st63} suppressor screen. (**G**) Workflow for primary small molecule screening of *gpr126*^{st63}*; mbp:gfp* larvae.

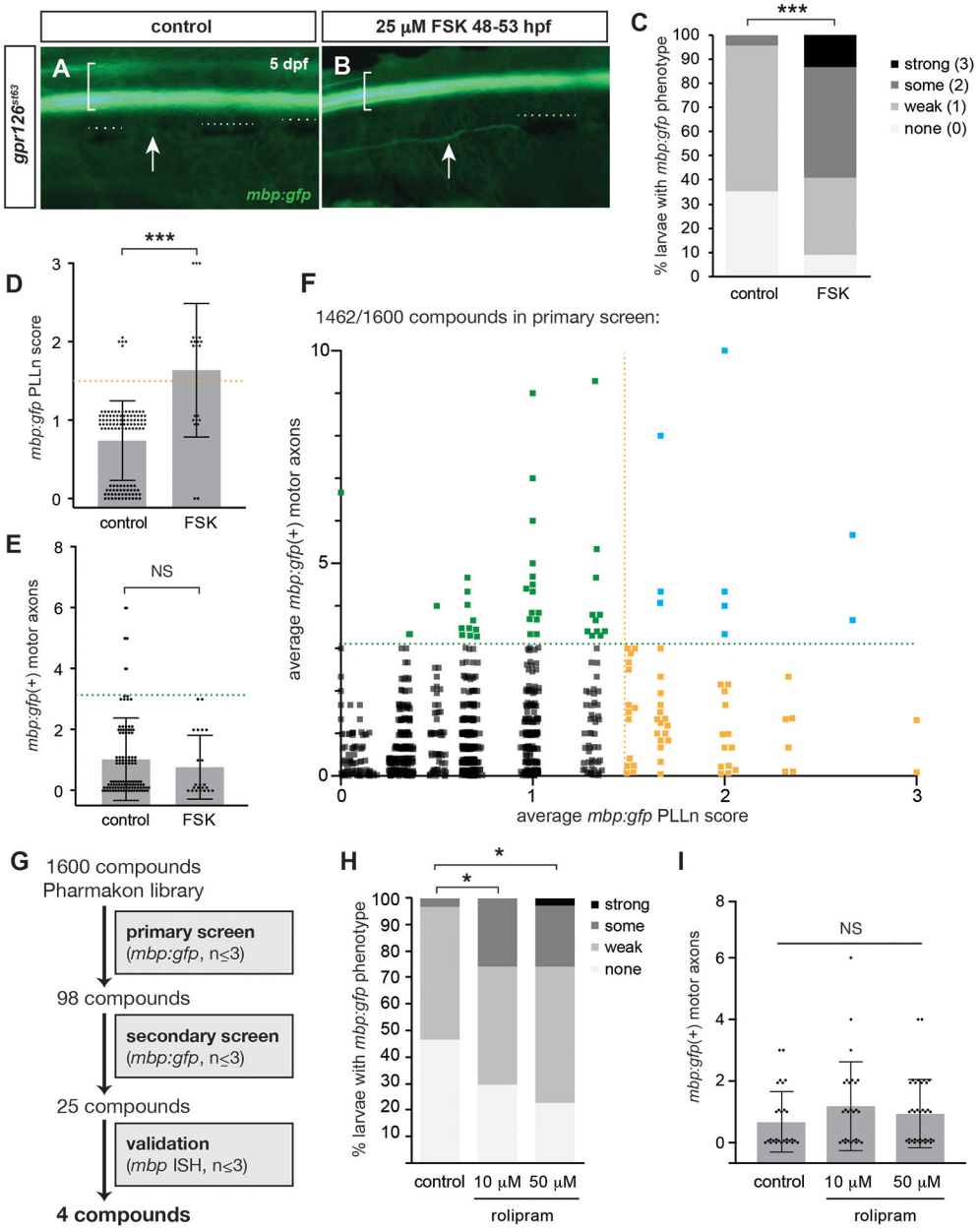

Figure 2. *In vivo* small molecule screening of *gpr126* hypomorphs reveals five suppressor compounds

(**A**) *mbp:gfp* expression in control and (**B**) 25 μM forskolin (FSK) pulsed *gpr126*^{st63} 5 dpf larvae. Brackets denote spinal cord, arrows indicate PLLn, dotted lines indicate melanocytes obscuring PLLn. (**C**) Quantification of *mbp:gfp* as a percentage of larvae with each *mbp* PLLn phenotype at 5-6 dpf. *** p<0.001, Fisher's Exact Test, "non-*st63*-like" vs "*st63*-like." (**D**) Transformation of data from panel **C**. Dots indicate individual larva and are jittered to show all samples. Bars indicate mean ± SD. *** p<0.001, Student's t-test. (**E**) Quantification of *mbp:gfp*(+) motor axons at 5-6 dpf. NS = no significant difference. (**F**) PLLn score and *mbp:gfp*(+) motor axons for 1462 Pharmakon compounds. Each square = one compound. Dots are jittered and transparent to show all samples. (**G**) Workflow of

screens for *gpr126*^{st63} suppressor compounds. (**H**) Rolipram restores PLLn *mbp:gfp* but not (**I**) motor axons in *gpr126*^{st63}. * p<0.05, Fisher's Exact Test, "non-*st63*-like" vs "*st63*-like".

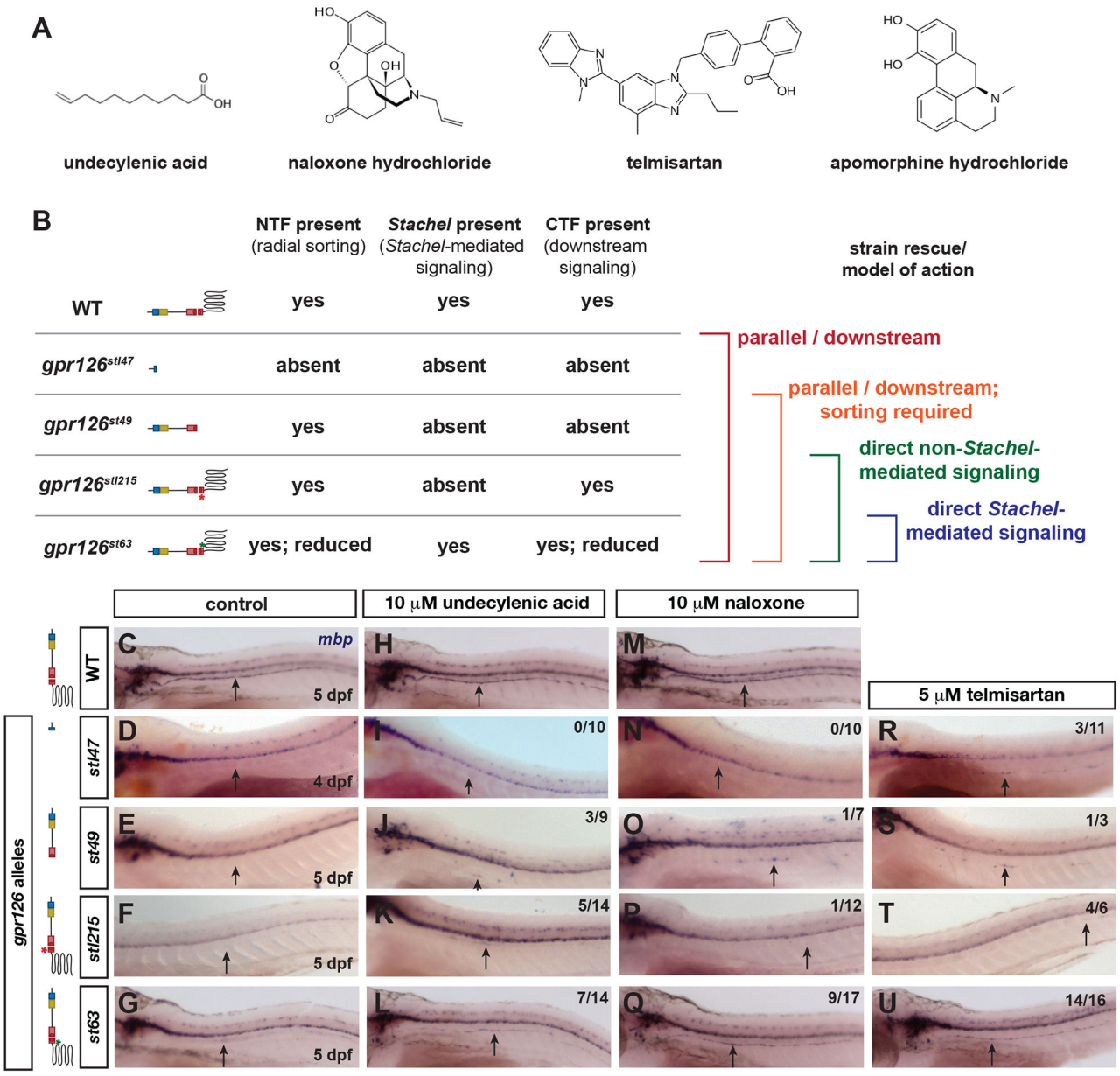

Figure 3. An allelic series of *gpr126* parses direct versus indirect compound function.

(**A**) Molecular structure for screen hits (PubChem). (**B**) Schematic of *gpr126* alleles, predicted proteins, phenotypes, and predicted drug functions based on *mbp* restoration. (**C-U**) Whole-mount *in situ* hybridization for *mbp* in wild-type (WT) or *gpr126*. Black arrows indicate PLLn. Fraction of *gpr126* larvae with increased *mbp* is noted in upper right of each image. (**C-G**) *mbp* expression in control larvae. Note absence of PLLn *mbp* in $gpr126^{stl47}$, $gpr126^{st49}$, and $gpr126^{stl215}$ (**D-F**) and reduction in $gpr126^{st63}$ (**G**). (**H-L**) PLLn *mbp* expression is partially restored in $gpr126^{st49}$ (**J**), $gpr126^{stl215}$ (**K**), and $gpr126^{st63}$ (**L**) in 10 μM undecylenic acid. (**M-Q**) PLLn *mbp* is weakly increased in one larva for $gpr126^{st49}$ (**O**) and $gpr126^{stl215}$ (**P**) but strongly increased in $gpr126^{st63}$ (**Q**) with 10 μM naloxone. (**R-U**) *mbp* PLLn expression is increased across all alleles in 5 μM telmisartan-treated larvae.

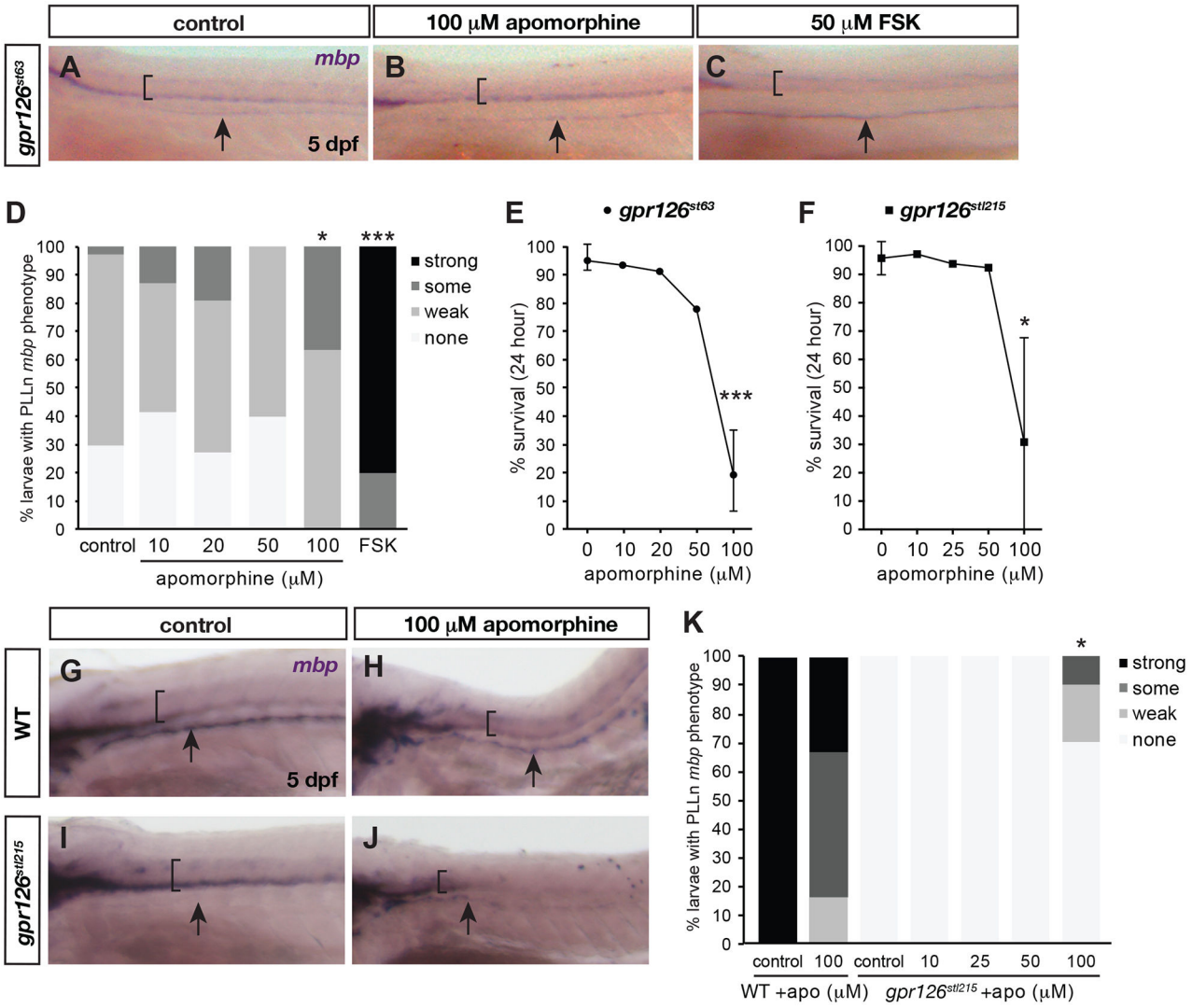

Figure 4. Apomorphine hydrochloride suppresses *gpr126* hypomorphic phenotype at high doses.

(**A-C, G-J**) Whole-mount *in situ* hybridization for *mbp* in PLLn of *gpr126*^{st63} (**A-C**) or *gpr126*^{stl215} (**G-J**) with control, apomorphine, or forskolin (FSK) treatment at 5 dpf. Black arrows indicate PLLn. (**D, K**) Quantification expressed as a percentage of larvae with each *mbp* PLLn phenotype at 5 dpf. * p<0.05, *** p<0.001, Fisher's Exact Test, "wild-type" vs. "mutant" (*gpr126*^{st63} or *gpr126*^{stl215}) categories for treated vs. control. (**E-F**) Survival curve following 24-hour treatment with indicated concentrations of apomorphine. Dots indicate mean ± SD % alive across technical replicates. *** p<0.001, 0 vs.100 μM apomorphine. Sample numbers in Detailed Methods.

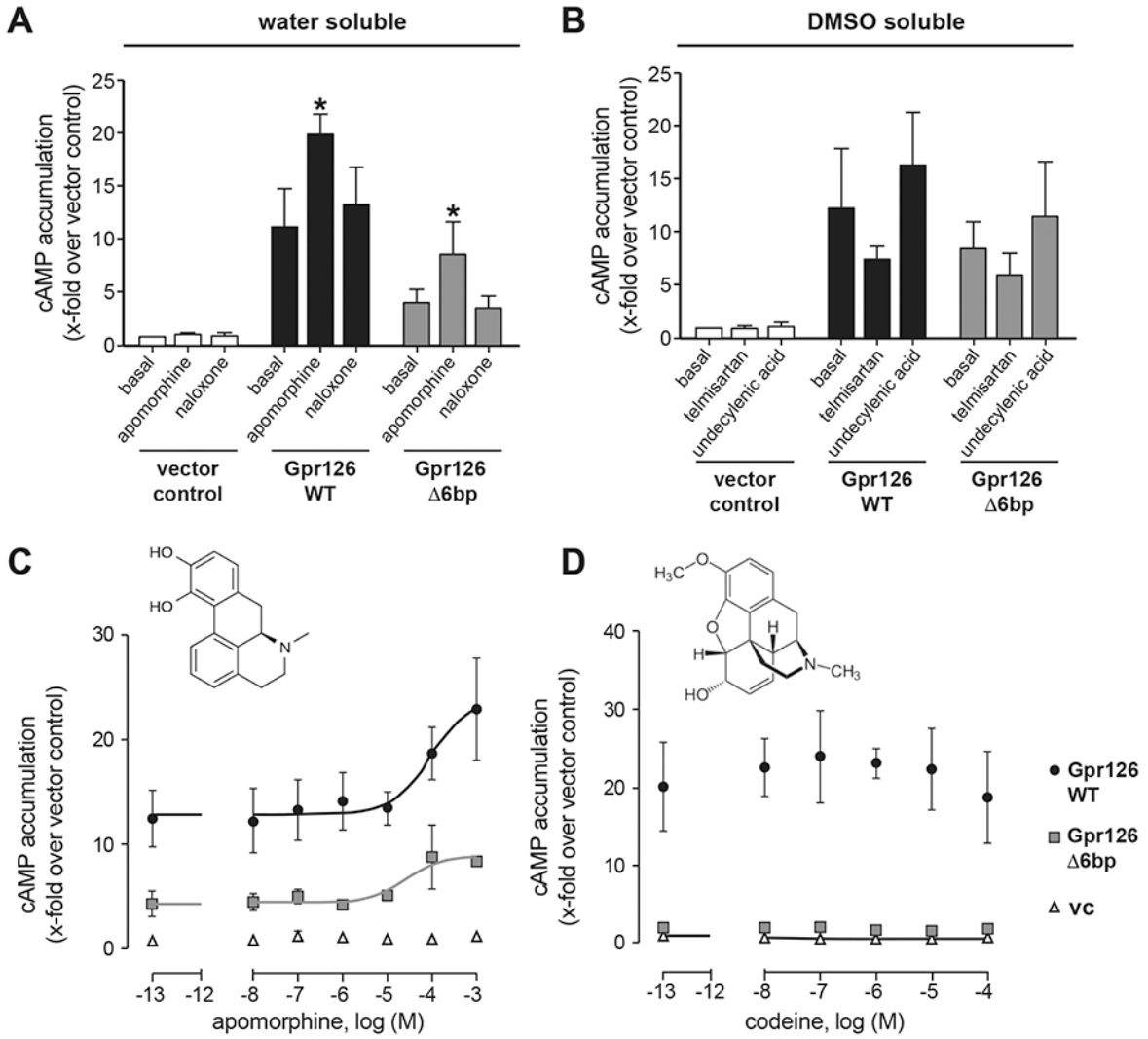

Figure 5. Apomorphine hydrochloride is a direct activating ligand for Gpr126.

(**A-B**) COS-7 cells were transiently transfected with empty vector, WT and mutant (Δ6bp lesion as in *gpr126*^{stl215}) zebrafish *gpr126* plasmid, and cAMP accumulation was measured after stimulation with given substances at 100 μM. Results are given as x-folds over vector control (vc: 1.0 ± 1.1 nM) (**A**) and vector control with 0.1 % DMSO (basal vc: 2.2 ± 3.1 nM) (**B**) for water and DMSO soluble substances, respectively. Bars show means ± SEM of three independent assays each performed in triplicates. * $p<0.05$, one-way ANOVA with Dunn's multiple testing for each substance induced activation vs. basal levels. (**C-D**) Concentration-response curve of apomorphine (EC_{50} WT: 21.5 μM Δ6bp mutant: 33.4 μM) (**C**) and codeine (no dose response detectable) (**D**). Results are given as x-folds over vector control (vc: 2.9 ± 0.6 nM) of four independent assays each performed in triplicates. Insets show structure of each molecule (PubChem).

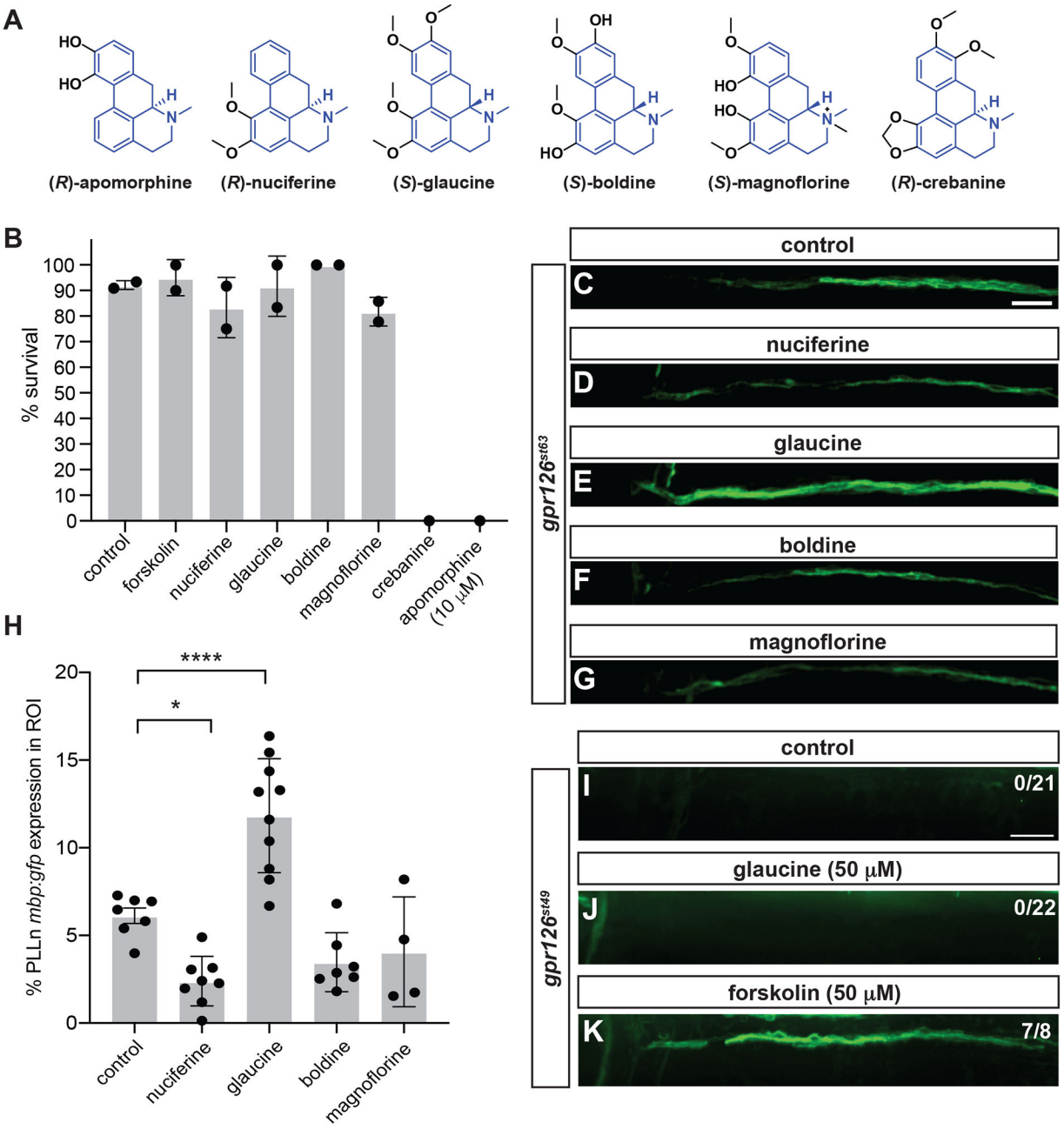

Figure 6. Glaucine suppresses *gpr126*^{st63} hypomorphic phenotype likely by direct interaction with Gpr126.

(**A**) Structures of aporphine compound series. Core scaffold highlighted in blue. (**B**) Toxicity screening of aporphines from 47-54 hpf. Survival was assessed at 54 hpf. All compounds were at 50 μM unless otherwise noted. Control, 1% DMSO. n≥10 in all cases. (**C-G, I-K**) PLLn *mbp:gfp* expression in 5 dpf *gpr126*^{st63} (**C-G**) or *gpr126*^{st49} (**I-K**) following 50 μM compound treatment at 47-54 hpf. Indicated region is the most anterior portion of the PLLn. Scale bar, 25 μm. Control, 1% DMSO. Note increased PLLn *mbp:gfp* expression in *gpr126*^{st63} treated with glaucine (**E**) compared to control (**C**) but absence of *mbp:gfp* in glaucine-treated *gpr126*^{st49} (**J**). (**H**) Quantification of PLLn *mbp* expression within ROI of

gpr126^{st63} larvae in **C-G**. Bars indicate means ± SD. ****p<0.0001, *p<0.05, one-way ANOVA with Dunnett's multiple testing for each compound against control.

Table 1:

mbp expression in larvae treated with small molecules used in primary, secondary, and validation screens

	Primary Screening (*mbp:gfp*)			Secondary Screening (*mbp:gfp*)		Validation with ISH	
	average *mbp:gfp* PLLn score	**average *mbp:gfp* motor nerves**	**n=**	**# increased PLLn *mbp:gfp* (score > 2) out of n**	**average *mbp:gfp* motor nerves**	**# increased PLLn *mbp:gfp* (score > 2) out of n**	**Hit for allelic series test?**
control (DMSO, untreated)	0.7	1	113	0/3	1.3	0/2	n/a
forskolin pulse	1.6	0.7	22	3/3	2.3	3/3	n/a
GPCR binding							
apomorphine hydrochloride	**1.7**	0.7	3	**1/2**	0.5	ND *	**yes** *
telmisartan	1	**6**	3	**1/3**	4	**1/2**	**yes**
naloxone hydrochloride	**1.7**	**8**	3	0/3	**3.3**	**2/3**	**yes**
tolazoline hydrochloride	**1.7**	0	3	0/3	**3.4**	0/3	
oxelaidin citrate	**1.5**	0	2	**1/3**	1.7	0/3	
norgestrel	**2**	0.7	3	**1/3**	0	0/2	
cAMP elevator							
rolipram	**2.3**	1	3	**1/3**	3	**1/3**	PDE inhibitor
steroids/hormones							
triamcinolone acetonide	**3**	0	3	0/3	**3.7**	0/3	
levothyroxine	**2**	**10**	1	**1/3**	**4.7**	0/2	
analgesic							
glafenine	1.3	**4.7**	3	**1/3**	1	0/3	
other nervous system modulator							
duloxetine hydrochloride	**1.5**	3	2	**1/3**	3	0/3	
isaxonine	0.7	**4.3**	3	**1/3**	1	0/3	
aceglutamide	**1.7**	**1.7**	3	0/2	**4.5**	0/2	
antibacterial							
ceforanide	1.3	**3.3**	3	**1/3**	1.7	0/3	
betamipron	0.7	**4.7**	3	0/3	**3.3**	0/3	
chlortetracycline hydrochloride	0.7	**3.3**	3	**1/3**	2.7	0/3	
antifungal/antihelminthic							
acedapsone	**1.7**	1.3	3	**1/3**	2.3	0/1	

	Primary Screening (*mbp:gfp*)			Secondary Screening (*mbp:gfp*)		Validation with ISH	
	average *mbp:gfp* PLLn score	**average *mbp:gfp* motor nerves**	**n=**	**# increased PLLn *mbp:gfp* (score > 2) out of n**	**average *mbp:gfp* motor nerves**	**# increased PLLn *mbp:gfp* (score > 2) out of n**	**Hit for allelic series test?**
oxfendazole	**2.7**	**5.7**	3	**1/3**	2.3	0/3	
undecylenic acid	1	**4.3**	3	**1/3**	2	**1/2**	**yes**
artemether	**1.7**	1	3	**5/12** **	**11**	0/10 **	
antineoplastic							
azacitidine	1.3	**3.3**	3	0/3	**4**	0/3	
other							
sodium gluconate	1	**3.3**	3	0/3	**3.3**	0/3	
tetroquinone	1.3	**5.3**	3	0/3	**6**	0/3	
allantoin	**1.5**	2.5	2	0/3	**3.3**	0/1	
benurestat	1	**4.5**	2	**1/3**	1	0/2	

* Apomorphine-treated larvae did not survive re-screening; however, subsequent *in vivo* assays are reported in Fig. 4 and *in vitro* assays in Fig. 5.

** New drug stock was used (rather than Pharmakon library) in larger culture dish, see Methods